

Comparative Study of 3-Dimensional Woven Joint Architectures for Composite Spacecraft Structures

Justin S. Jones, Daniel L. Polis, Russell R. Rowles, Kenneth N. Segal
National Aeronautics and Space Administration
Goddard Space Flight Center
Greenbelt, MD 20771

ABSTRACT

The National Aeronautics and Space Administration (NASA) Exploration Systems Mission Directorate initiated an Advanced Composite Technology (ACT) Project through the Exploration Technology Development Program in order to support the polymer composite needs for future heavy lift launch architectures. As an example, the large composite structural applications on Ares V inspired the evaluation of advanced joining technologies, specifically 3D woven composite joints, which could be applied to segmented barrel structures needed for autoclave cured barrel segments due to autoclave size constraints. Implementation of these 3D woven joint technologies may offer enhancements in damage tolerance without sacrificing weight. However, baseline mechanical performance data is needed to properly analyze the joint stresses and subsequently design/down-select a preform architecture. Six different configurations were designed and prepared for this study; each consisting of a different combination of warp/fill fiber volume ratio and preform interlocking method (Z-fiber, fully interlocked, or hybrid). Tensile testing was performed for this study with the enhancement of a dual camera Digital Image Correlation (DIC) system which provides the capability to measure full-field strains and three dimensional displacements of objects under load. As expected, the ratio of warp/fill fiber has a direct influence on strength and modulus, with higher values measured in the direction of higher fiber volume bias. When comparing the Z-fiber weave to a fully interlocked weave with comparable fiber bias, the Z-fiber weave demonstrated the best performance in two different comparisons. We report the measured tensile strengths and moduli for test coupons from the 6 different weave configurations under study.

1. INTRODUCTION

1.1 Purpose

Composite structures in heavy-lift launch vehicles are projected to be the largest composite structures ever built for aerospace applications. Some of these composite shelled structures are projected to be larger than 9 meters in diameter and greater than 10 meters in length. Because these structures exceed current autoclave sizes, one must consider options such as expansion of autoclave infrastructure, development and qualification of out-of-autoclave technologies [Ref 1], or advanced joining technologies.

To this end, NASA's Advanced Composites Technologies (ACT) program seeks to develop advanced composite material solutions for the aforementioned structures. One step in this direction is the development of 3D woven H-preform joints for connecting large barrel segments. These H-preforms could serve as longitudinal joints, connecting traditionally manufactured

(autoclave cured in existing autoclaves) barrel segments. In this application, 3D woven joints may improve the damage tolerance of the longitudinal joints relative to more traditional double lap joints, essentially increasing reliability without sacrificing weight. Figure 1 shows a traditional double lap joint, as recently implemented on the NASA Engineering and Safety Center's (NESC) Composite Crew Module, versus a 3D woven H-preform replacement, as shown in a joint coupon in Figure 2.

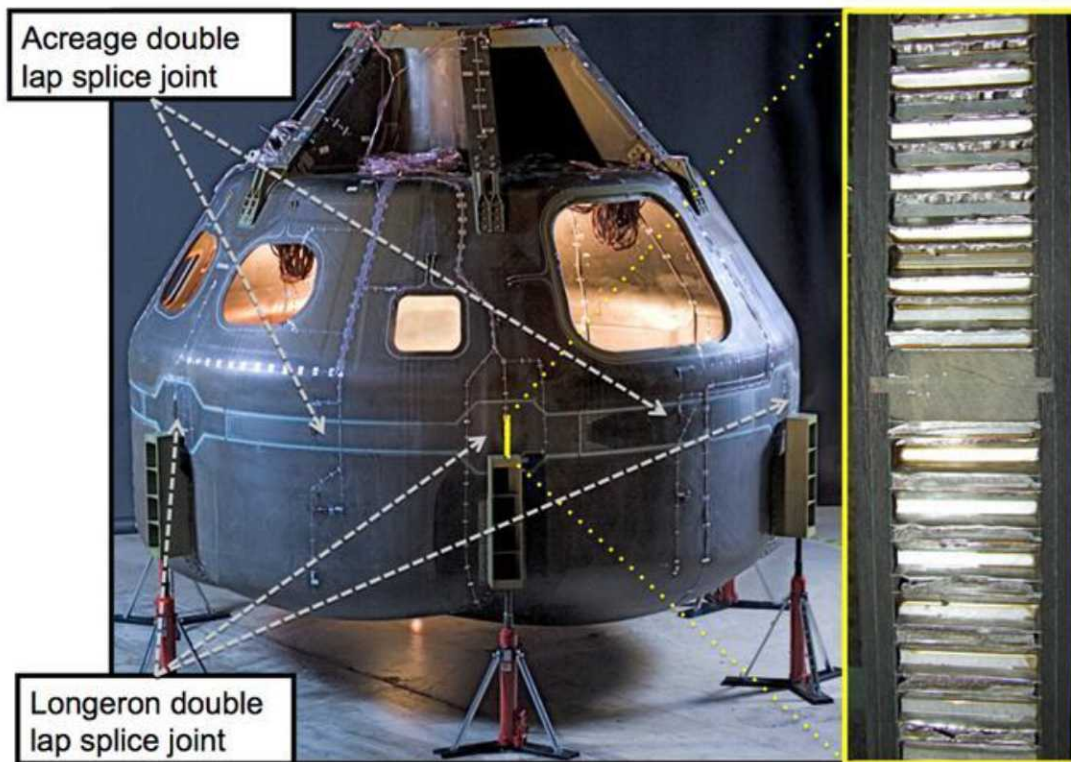


Figure 1: NASA Engineering and Safety Center's (NESC) Composite Crew Module, showing a traditional double lap splice joint of upper and lower sandwich shells.



Figure 2: 3D woven H-preform joint coupon of two inch thick sandwich.

Prior to designing and implementing a full-scale H-preform joint, baseline mechanical performance data is needed to properly down-select the weave architecture. Toward this end, this study evaluates six different weave designs; each with a different combination of warp/fill fiber tow volume ratio and through-thickness interlocking. This paper reports the measured tensile strengths and moduli for test coupons from these weave configurations under study. Values are reported for both the fill fiber direction of the H-preform cap surface and the warp fiber direction of the cap surface (see Section 2.1 for direction definition).

1.2 Overview of Weave Configurations

The six 3D weave configurations of interest in this study involve varying warp to fill fiber ratios and one of three general through-thickness weave architectures. Each H-preform configuration consists of two faces, or caps, each with 6 layers of IM7 fiber (PAN-based, intermediate modulus carbon fiber produced by Hexcel, 12K filament count tows) that are coupled together with a thin web section that creates the H-shape. The two main through-thickness weave architectures are “Fully Interlocked” and “Z-fiber”. Generically, these interlocking methods are shown schematically in Figure 3. The fully interlocked weave has each layer bound to its neighbor with a fill tow that crosses over or under every warp tow. The Z-fiber design achieves through-thickness interlocking through a Z-tow that passes straight through the thickness of the cap layup. This method allows both warp and fill tows to remain nearly straight. A third architecture, used in Weave 2, is denoted as the “Hybrid” architecture. However, it shares more character with the fully interlocked weave, as the warp fiber is used to interlock adjacent layers, but is done so at a different interlocking frequency. This produces more straight runs of warp fiber. A summary of the weave configurations is provided in Table 1.

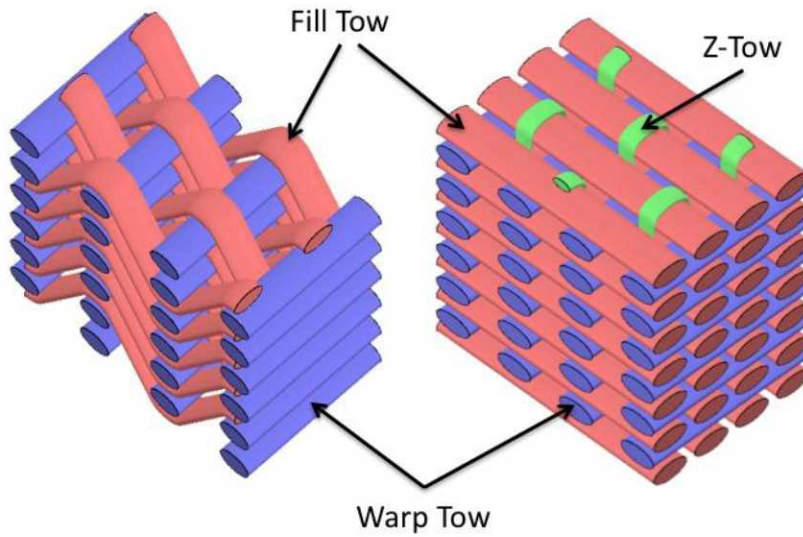


Figure 3: Generic representation of the interlocking methods: Fully interlocked (left) and Z-fiber (right).

Table 1: Description of the six weave architectures used in this study.

Weave #	Warp/Fill Fiber Ratio	Architecture
1	50/50	Fully Interlocked
2	50/50	Hybrid
3	50/50	Z-fiber
4	25/75	Z-fiber
5	75/25	Z-fiber
6	25/75	Fully Interlocked

Prior to the testing reported in this article, all of the H-preforms were fully infused and cured with MTM®45-1 resin, which is a toughened epoxy produced by Advanced Composites Group. Figure 4 contains an image of Weave 1 prior to resin infusion. All the performs were woven by Bally Ribbon Mills (Bally, PA).

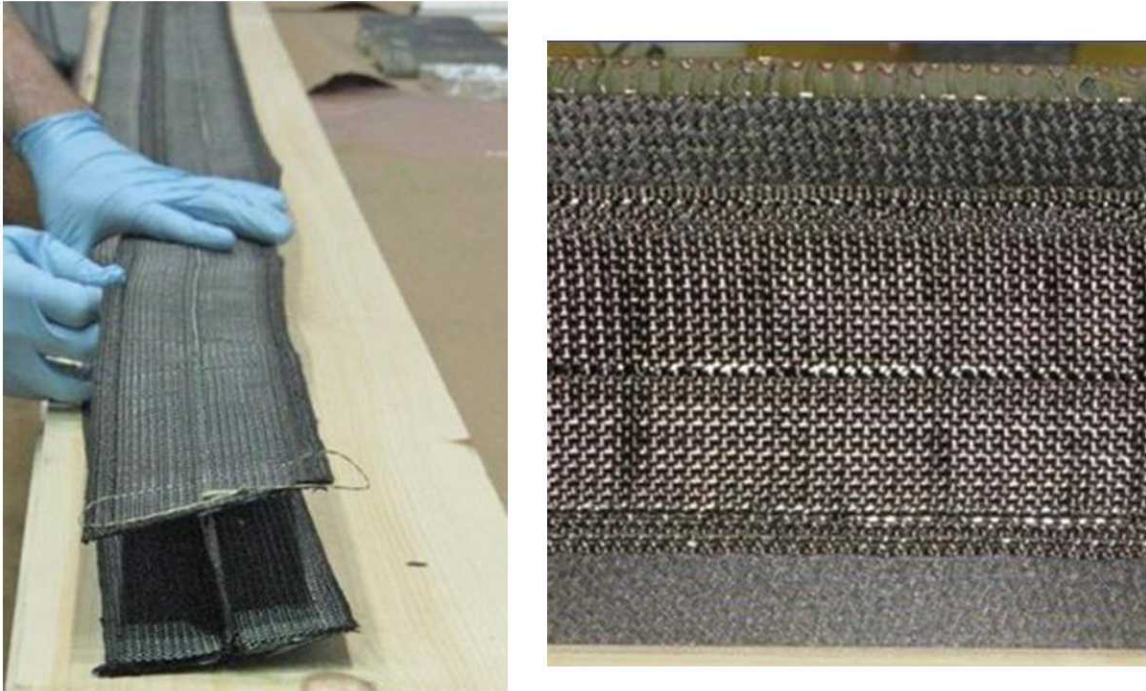


Figure 4: Example of an H-preform prior to resin infusion. The image on the left shows the full preform and the right image shows the cap of a fully interlocked preform on top of a cured composite sandwich panel.

2. EXPERIMENTATION

2.1 Sample Preparation

In order to obtain H-preform specimens for characterization, each unique weave was infused and cured in a single step. Rather than infusing and curing with sandwich panels inserted into the H-preform, as shown in Figure 2, release coated tooling was used. This enabled the joining process to be simulated but produced a free-standing cured H-preform coupon. These infusion coupons were produced in lengths of approximately eight inches. These coupons were sectioned into 1" wide samples using a Struers Exotom-M chop saw. For each of the H-preforms, samples were sectioned so that at least 4 coupons were extracted from the cap in the warp fiber direction and at least four samples were extracted from the cap—across the joint—in the fill fiber direction. Figure 5 shows a 1" wide cross-section of a free-standing H-preform that provided two fill direction coupons, which were released from one another by cutting the thin web section that connects them. For illustration, the warp fiber direction is also noted in the image. For the warp direction samples, the sections were chosen such that they excluded the tapered edges and areas within $\frac{1}{4}$ " from the web.

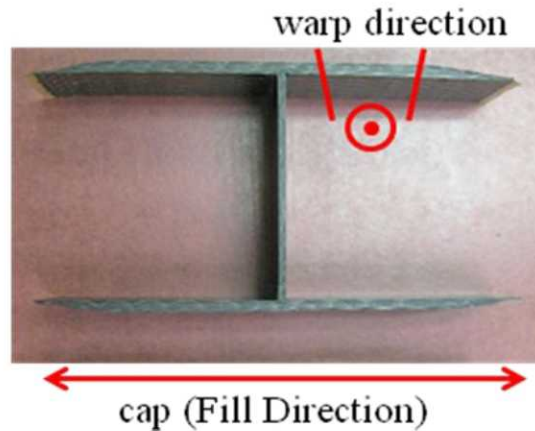


Figure 5: Cross-section of H-preform showing the fill and warp fiber directions that were isolated during mechanical tests.

Once the samples were sectioned, grip tabs were applied by bonding 1" x 1" x 1/16" thick G10 composite to both sides of each end of the samples using Hysol® EA 9309.2 epoxy. The epoxy was cured at 80°C for 1 hour. The sides of the samples were then lightly sanded to remove any excess epoxy or irregularities. Lastly, the front surface was painted with a black and white stochastic speckle pattern for the purpose of providing a surface that could be tracked for strain imaging purposes, as described in Section 2.2. A completed fill direction sample and warp direction sample are shown in Figure 6. The speckle pattern can be seen on the top surface of the warp direction sample. Sample dimensions, particularly widths and thicknesses, were then measured and recorded.

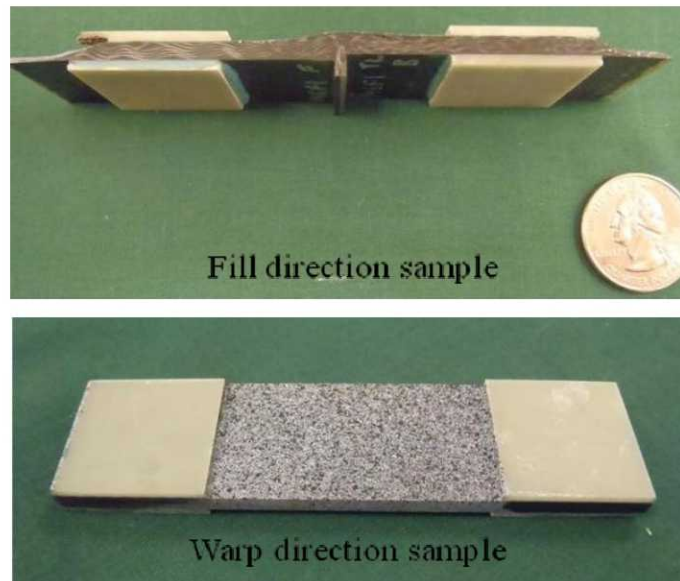


Figure 6: Completed fill and warp direction samples. In the upper image, the remaining fragment of the web section can be seen in the center of the sample.

2.2 Equipment

To determine the strain, digital image correlation (DIC) was performed using an Aramis strain visualization system. The DIC technique measures strain directly from the sample, completely independent of any compliance that may exist throughout the test system. DIC measures strain via tracking of identifiable features on the sample (or on the grips) throughout the image sequence. The stochastic pattern that was sprayed onto these samples provided the locally unique contrast and texture through which a superimposed grid of markers in the software was able to track the surface deformation. Since this is a full-field strain measurement, local strain and modulus information from anywhere on the deformed surface can be gleaned. This technique is particularly useful in this study since the thicknesses and fiber-derived constitutive properties vary greatly across the gauge sections. The Aramis system consists of two cameras, two light sources and a software-based geometric calibration which incorporates the precise relative angles and focal distances of the cameras to provide 3-dimensional displacement information. The prepared samples were tested using an Instron® 4485 electromechanical universal testing system equipped with a 20,000 lb load cell. An image of the system is shown in Figure 7.

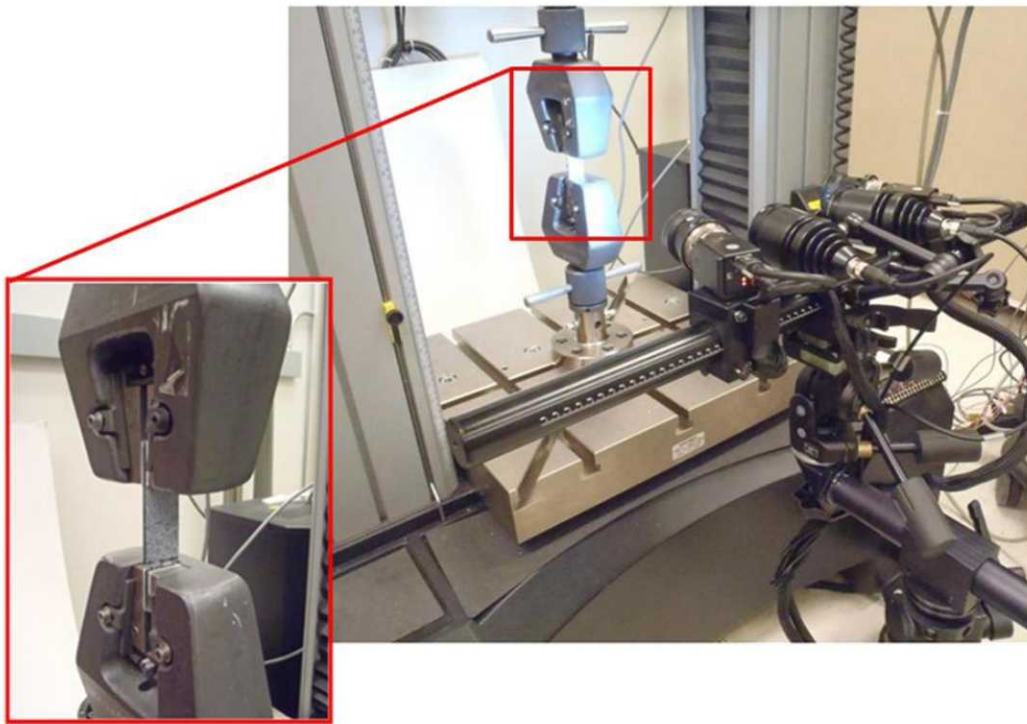


Figure 7: Mechanical test system showing sample loaded into the grips (inset) and the Aramis™ DIC system placed in front of the test region.

2.3 Test Procedure

During the test, the DIC system captured images at a rate of one frame per second. Load data was also collected simultaneously through the Instron® load cell and was later correlated with

the strain data. The samples were loaded at a constant displacement rate of 0.127 cm/min (0.05 in/min) until failure.

2.4 Analysis

To determine the total strain for a given sample, the DIC local surface strain (specifically, the component of strain along the loading direction) was averaged across a selected region. For the warp direction coupons, the entire surface between the grips was averaged and reported as one value. Regions of poorly tracked cells along edges or near grip epoxy lines were excluded. An example of this strain selection for a warp direction sample is shown in Figure 8.

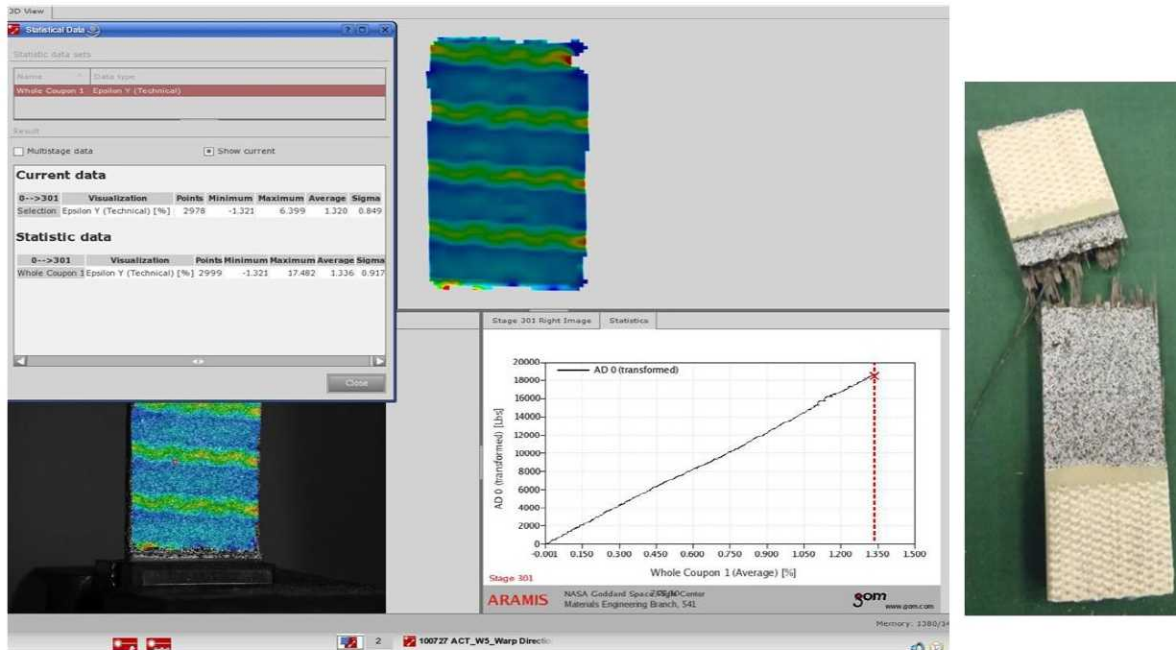


Figure 8: Screen capture of software showing the strain in the loading (warp) direction superimposed on the sample (lower left), the mean value statistic from the selected region (taken from the full DIC surface in this case), and statistical plot showing the load versus the mean strain. The image to the right shows the actual sample after failure.

For the fill direction coupons, the strain was computed for the flats on both sides of the joint. The center of the coupon, i.e. the joint between the cap and web, was not included in either measurement as this region would have a local thickness and properties distinct from the adjoining flats which would affect subsequent modulus calculations. An example of this strain selection for a fill direction sample is shown in Figure 9.

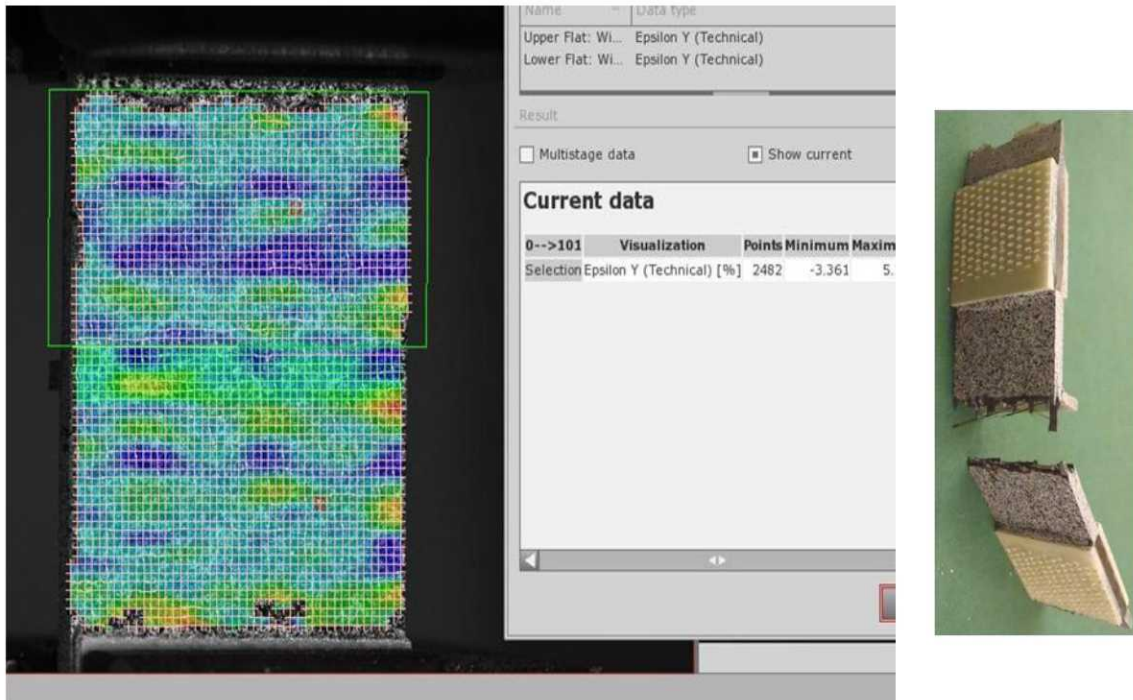


Figure 9: Screen capture of software showing the strain in the loading (fill) direction superimposed on the sample. For the fill direction samples, the mean value statistics from both sides of the joint were collected (note box outlining the upper flat). The image to the right shows the actual sample after failure.

The ultimate tensile strength (UTS) was determined for each coupon by dividing the measured load at failure by the average cross-sectional thickness. Since the fill direction coupons had some degree of thickness variation across the web, some error may be incorporated in this measurement; however, we expect this error to be minimized by the fact that the thickness variation was due to resin content as opposed to ply drops or weave variation. The modulus was calculated for each sample by taking the slope of the linear portion of the stress-strain plot, between 0.1 - 0.3% (1000 – 3000 $\mu\text{m}/\text{m}$) strain. The warp direction coupons provided one modulus per specimen; whereas the fill direction specimens yielded a modulus from both sides of the joint.

3. RESULTS

3.1 Individual Test Results

Individual profiles of the engineering stress versus the DIC spatially averaged strain are shown in the following figures. For each weave configuration, all samples in both the warp and fill fiber direction are provided. Noise inherent to the data collection hardware resulted in undesired oscillations in the load data for many of the plots. Filtering of the data to remove these oscillations caused aliasing because the noise frequency varied. Also the noise did not affect the modulus or UTS calculations; therefore the data is presented here in its unfiltered form. Warp direction specimens are shown in blue and have the highest overall strength for all weave

configurations except the 25/75 warp/fill fiber ratio samples: Weave 4 and Weave 6. As these samples are biased to have higher tow volumes in the fill direction, this is expected. For each fill direction specimen, the stress-strain profile is split into two components; the high strength side of the web is shown in red and the low strength side of the web is shown in green. All weaves except perhaps the hybrid Weave 2 show a recognizable asymmetry across the joint.

The Z-fiber architectures demonstrated a high level of linearity in both the warp and fill direction testing. Significant plasticity was observed, especially for the fill direction coupons, for all of the interlocked (including hybrid) weave architectures.

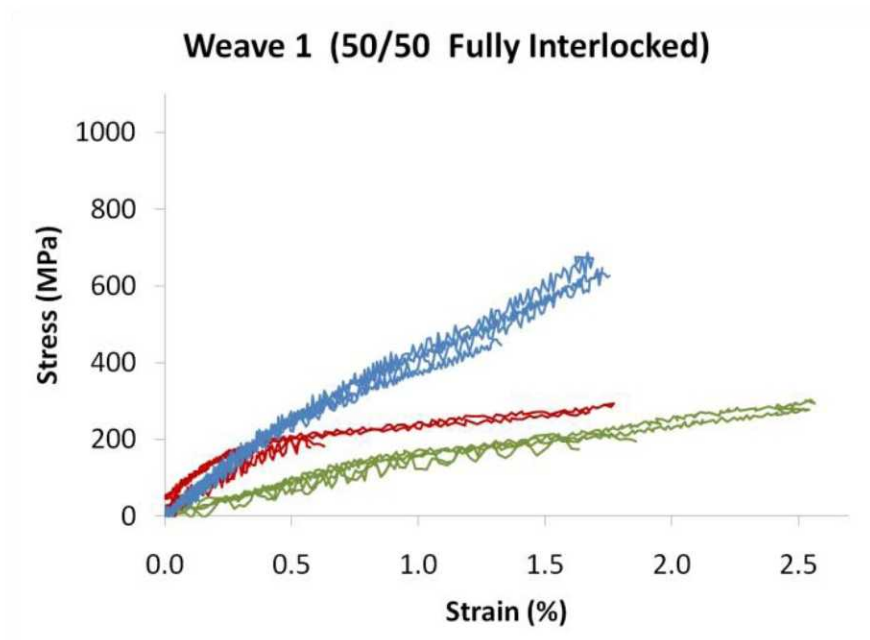


Figure 10: Engineering stress versus DIC spatially averaged strain for the fully interlocked Weave 1 preform with 50/50 warp/fill fiber bias. Warp direction specimens are shown in blue. The high strength side of the each fill direction specimen is shown in red and the low strength side is shown in green.

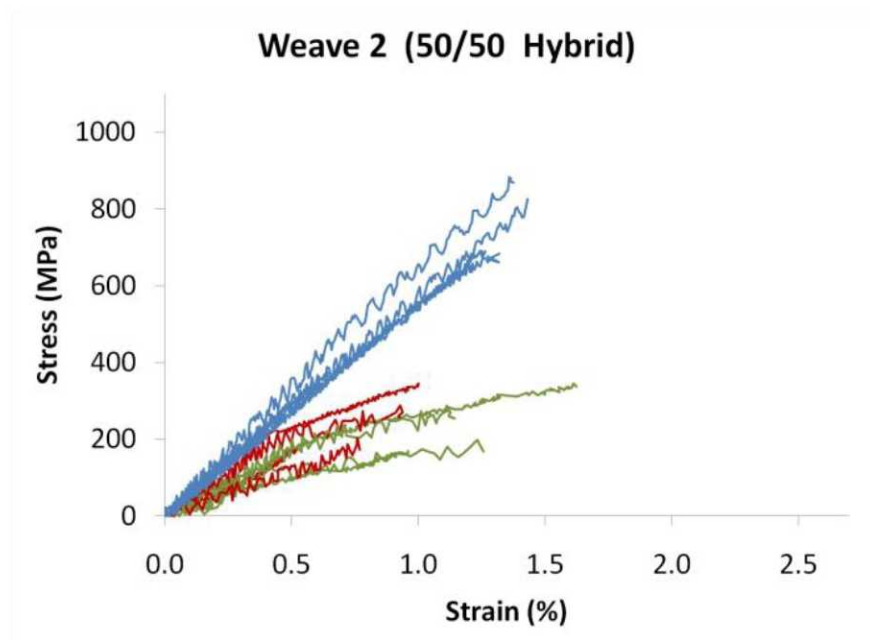


Figure 11: Engineering stress versus DIC spatially averaged strain for the hybrid Weave 2 preform with 50/50 warp/fill fiber bias. Warp direction specimens are shown in blue. The high strength side of the each fill direction specimen is shown in red and the low strength side is shown in green.

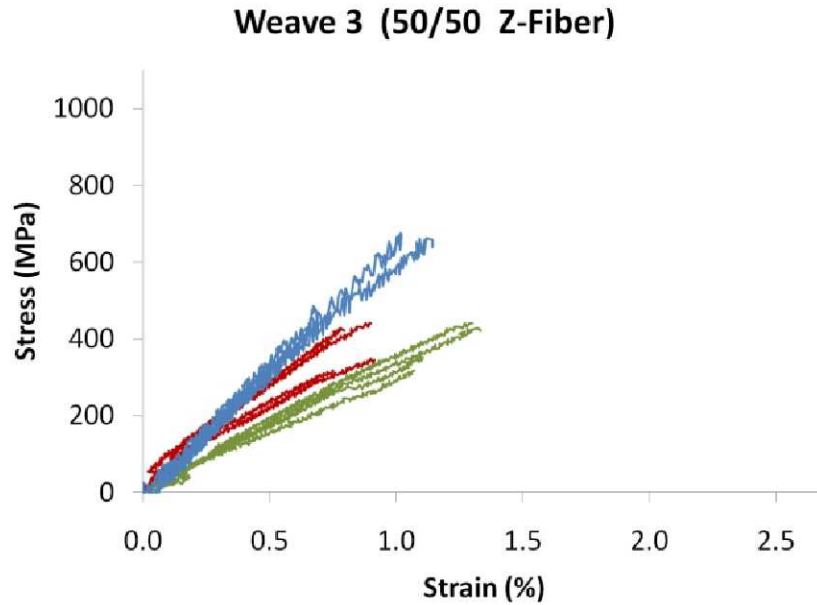


Figure 12: Engineering stress versus DIC spatially averaged strain for the z-fiber interlocked Weave 3 preform with 50/50 warp/fill fiber bias. Warp direction specimens are shown in blue. The high strength side of the each fill direction specimen is shown in red and the low strength side is shown in green.

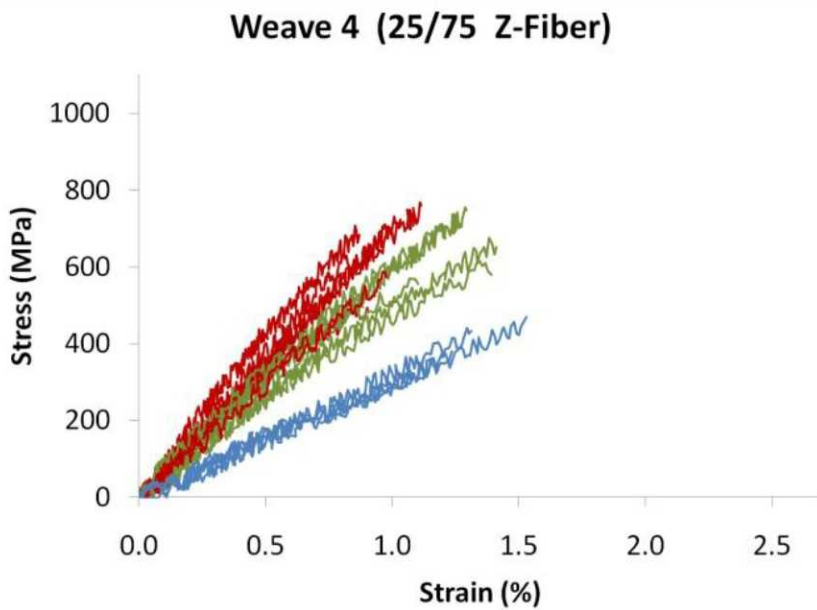


Figure 13: Engineering stress versus DIC spatially averaged strain for the z-fiber interlocked Weave 4 preform with 25/75 warp/fill fiber bias. Warp direction specimens are shown in blue. The high strength side of the each fill direction specimen is shown in red and the low strength side is shown in green.

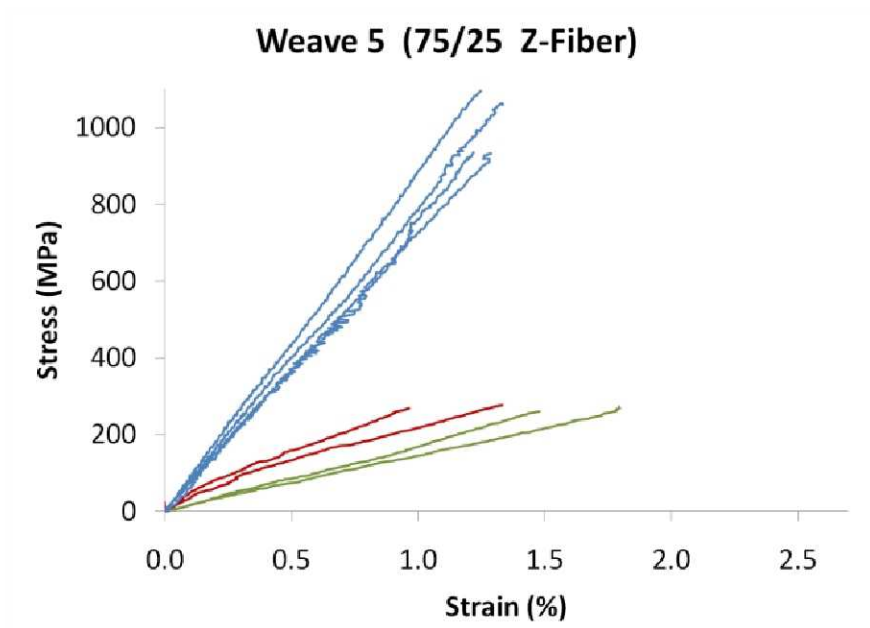


Figure 14: Engineering stress versus DIC spatially averaged strain for the z-fiber interlocked Weave 5 preform with 75/25 warp/fill fiber bias. Warp direction specimens are shown in blue. The high strength side of the each fill direction specimen is shown in red and the low strength side is shown in green.

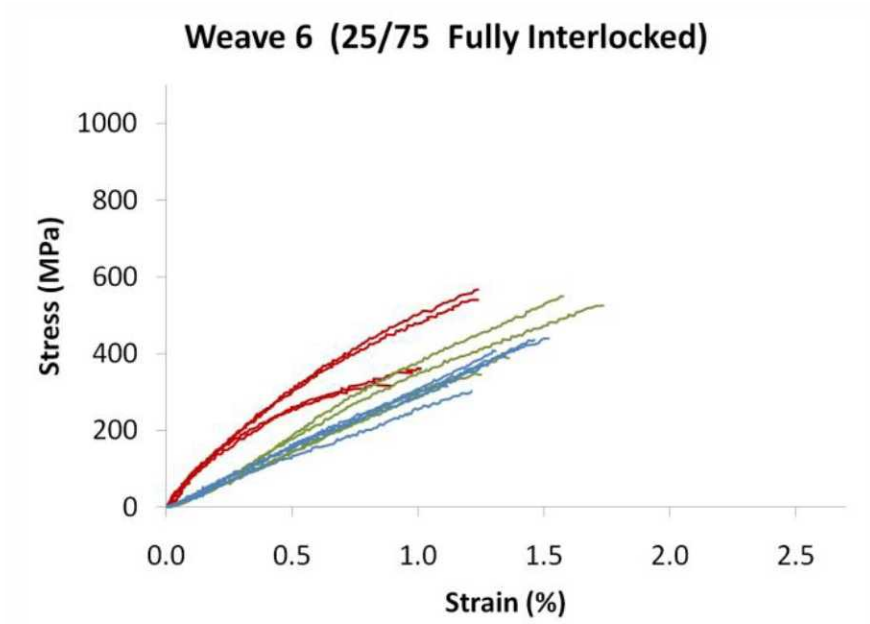


Figure 15: Engineering stress versus DIC spatially averaged strain for the fully interlocked Weave 6 preform with 25/75 warp/fill fiber bias. Warp direction specimens are shown in blue. The high strength side of the each fill direction specimen is shown in red and the low strength side is shown in green.

3.2 Weave Comparisons: Group Averages

The average moduli and ultimate tensile strengths for each coupon group (weave type and test direction) are given in Figure 16 and Figure 17, respectively. In order to compare warp and fill performance, the data is plotted in terms of fiber fraction in the direction that the particular test was performed. The moduli were determined over a 0.1 - 0.3% (1000 – 3000 $\mu\text{m}/\text{m}$) strain range, which was below any significant nonlinearity observed across all groups.

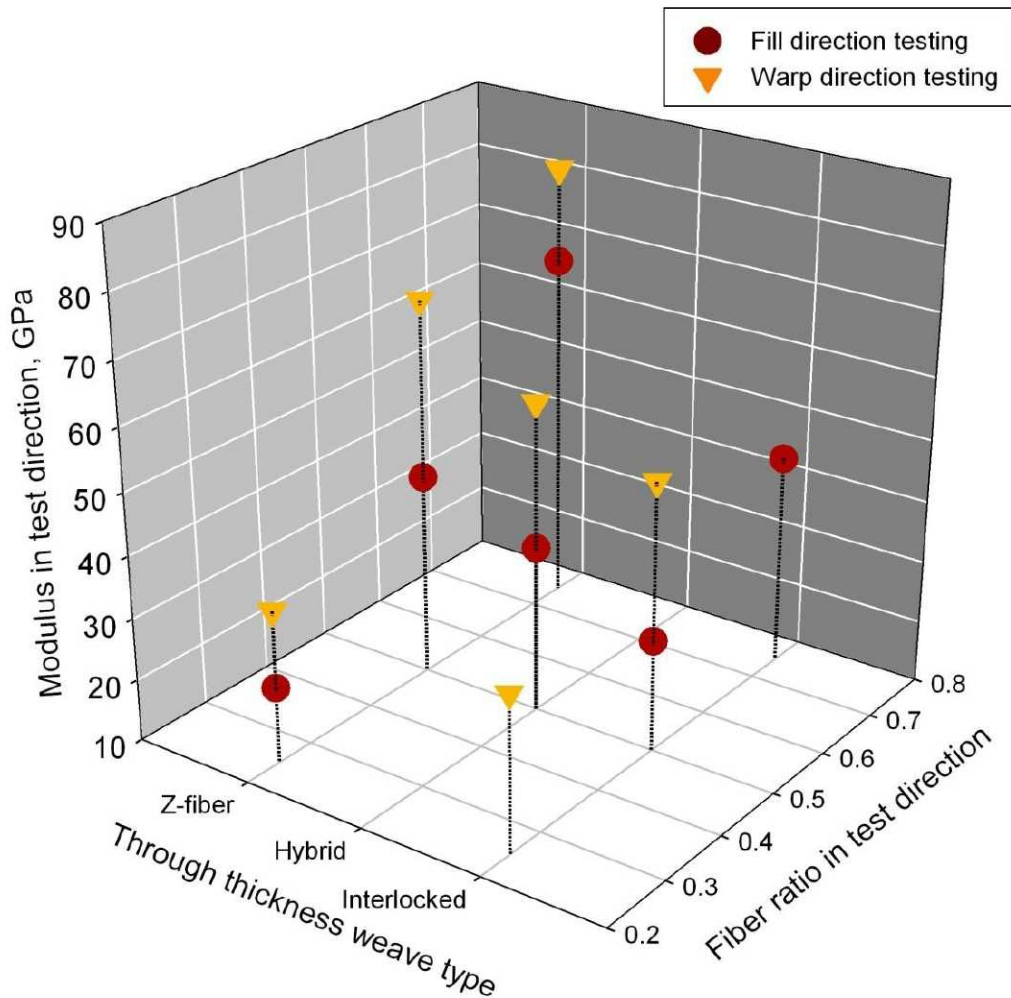


Figure 16: Group average elastic moduli for each weave type/test direction combination.

To first approximation, we expect the modulus in the testing direction to be proportional to the volume fraction of the fibers in the test direction. From Figure 16, two observations are readily apparent. The first is that the warp coupons are significantly stiffer than their fill direction counterpart, i.e. when compared at identical fiber fractions and weave types. This is anticipated for the fully interlocked weave and the hybrid weave since the fill fiber is used for the through-thickness interlocking. However, a similar effect is observed for the Z-fiber interlock, which

does not use the fill fiber for interlocking the layers. Therefore, this effect may also be an indication of fiber tensioning in the warp versus fill directions. The second observation is the considerable increase in stiffness, in both warp and fill testing, as we progress from fully interlocked to hybrid to Z-fiber. This trend is most clearly illustrated at the fiber fraction of 0.50. Essentially the sensitivity of through-thickness weave type on modulus is of similar magnitude to changing the fiber fraction from 0.25 to 0.75.

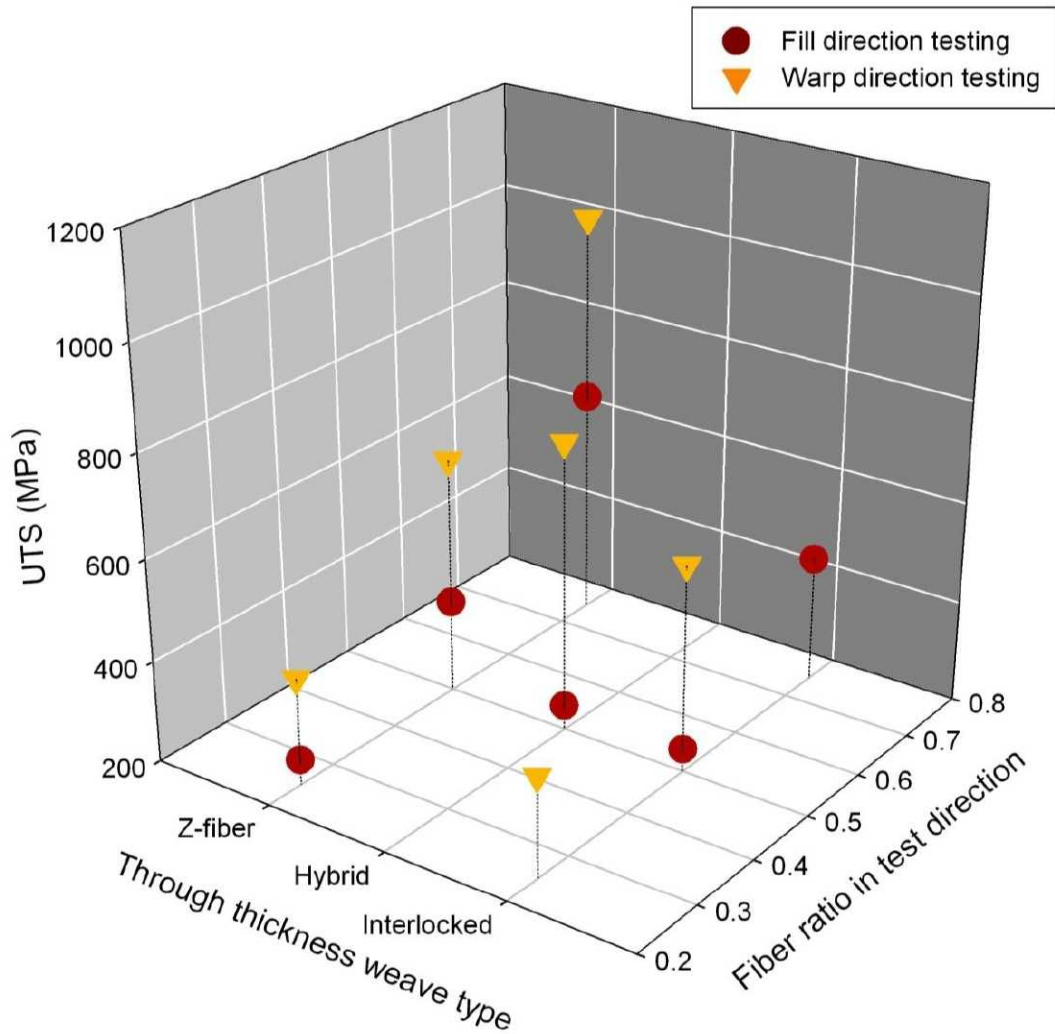


Figure 17: Group average UTS for each weave type/test direction combination.

Figure 17 shows a very similar trend for UTS as that described for modulus. Specifically, the warp direction coupons are significantly stronger than their fill direction counterparts and the effect of through thickness weave type is noticeable.

4. CONCLUSIONS

4.1 Weave Architecture Comparisons

As illustrated in Figure 16 and Figure 17, modulus and UTS show similar sensitivities to fiber architecture. Therefore, it is instructive to examine their relationship directly. Figure 18 shows UTS versus modulus (1000 – 3000 $\mu\text{m}/\text{m}$ strain range) for each coupon group average. All the data is described reasonable well with a single linear fit ($\text{UTS} = 10,746 \mu\text{m}/\text{m} * \text{modulus}$), despite the varying amount of nonlinear stress-strain behavior observed (Z-fiber behaving nearly linearly < hybrid < fully interlocked weave showing significant plasticity). Based on traditional composite material variation (2D laminated composite tested from various batches), 80% and 120% off of nominal behavior is typically sufficient for enveloping data scatter. These limits are also shown for reference and suggest that a maximum strain failure criterion is a reasonable preliminary design criterion for these 3D weaves in tension.

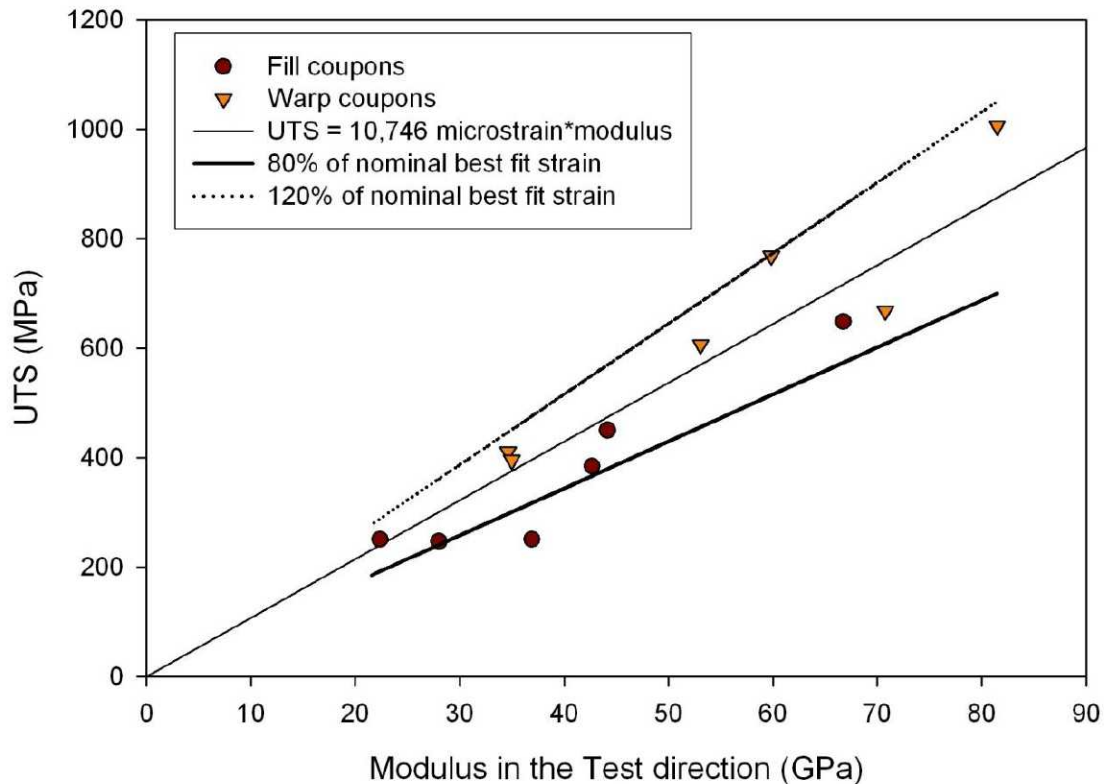


Figure 18: Group average ultimate tensile strength for each weave type/test direction combination.

As expected, the ratio of warp/fill fiber has a direct influence on strength and modulus. However, the effect of through-thickness architecture was stronger than anticipated. The weaves containing the Z-fiber architecture performed better overall than the fully interlocked weaves with comparable fiber bias: Weave 4 out-performs Weave 6 (each has 25/75 bias) and Weave 3 out-performs Weave 1 (each has 50/50 bias). In addition, the hybrid weave performs better overall than the fully interlocked weave with comparable fiber bias (though the strength values in

the fill direction are similar); Weave 2 out-performs Weave 1 (each has 50/50 bias). Future work should investigate the damage tolerance of H-preform joints to determine if the Z-fiber architecture retains as much strength-after-impact as the fully interlocked version.

5. REFERENCES

1. Sutter et. al., "Comparison of Autoclave and Out-of-Autoclave Composites", SAMPE 42nd ISTC - Salt Lake City, UT - October 11-14, 2010.